IOP Conf. Series: Materials Science and Engineering **202** (2017) 012047 doi:10.1088/1757-899X/202/1/012047

Study of Structural and Magnetic Properties of Silica and Polyethylene Glycol (PEG-4000)-Encapsulated Magnesium Nickel Ferrite ($Mg_{0.5}Ni_{0.5}Fe_2O_4$) Nanoparticles

F Deswardani, R Maulia and E Suharyadi

Department of Physics, Universitas Gadjah Mada, Sekip Utara BLS 21 Yogyakarta Indonesia

Email: esuharyadi@ugm.ac.id

Abstract. $Mg_{0.5}Ni_{0.5}Fe_2O_4$ has been successfully synthesized by using co-precipitation method. Two series of $Mg_{0.5}Ni_{0.5}Fe_2O_4$ silica encapsulated have been prepared by varying the concentration of silica and variation of PEG-4000 concentration. Analysis of X-Ray Diffraction (XRD) pattern showed that nanoparticles contained $Mg_{0.5}Ni_{0.5}Fe_2O_4$ spinel phase and γ-Fe_2O_3 phase with a particle size of 5.1 nm. The various of silica encapsulation give rise to produce a new phase of SiO_2 and increase the particle size to 16.1 nm. PEG-4000 encapsulation affected to create a new phase of γ-FeO(OH), and reduce the particle size down to 4.5 nm. Fourier Transform Infra Red (FTIR) for $Mg_{0.5}Ni_{0.5}Fe_2O_4$ showed absorption peaks around 300-600 cm^{-1} which are M-O bond vibration. After silica encapsulation, there was new bond vibration typical of silica such as Si-O-Si (1049.28 cm^{-1}), Si-OH (779.24 cm^{-1}), and Si-O-Fe (570.93 cm^{-1}). The PEG-4000 encapsulation creates a new vibration for typical of PEG-like of C-O (1103.28 cm^{-1}) and C-H (925.83, 1481.33, and 2924.09 cm^{-1}). Both of encapsulations series have M-O bond vibration indicating the presence of $Mg_{0.5}Ni_{0.5}Fe_2O_4$. After silica encapsulation, the coercivity of $Mg_{0.5}Ni_{0.5}Fe_2O_4$ decreased from 47 Oe to 10 Oe due to the decrease of particle size. Even though, the discrepancy of particle size as the effect of PEG-4000 encapsulation, the coercivity just slightly reduced to 46 Oe. The saturation magnetization of $Mg_{0.5}Ni_{0.5}Fe_2O_4$ decreased from 4.7 emu/g to 1 emu/g after silica encapsulation because diamagnetic SiO_2. Otherwise, the saturation magnetization increased to 7.7 emu/g after PEG-4000 encapsulation because of domination of $Mg_{0.5}Ni_{0.5}Fe_2O_4$ phase ratio.

Keywords: Magnesium nickel ferrite ($Mg_{0.5}Ni_{0.5}Fe_2O_4$), coprecipitation, encapsulation, silica, PEG-4000

1. Introduction

Recently, research on magnetic nanoparticles (MNPs) has been extensively done. The magnetic nanoparticles have quantum size effect (the transition region between atoms and bulk), and the large surface area dramatically changes some of the magnetic properties and exhibits superparamagnetic phenomena [1]. Spinel ferrite is one of the most important magnetic nanoparticles because their structure, chemical, electrical, and magnetic properties make them ideal for many applications. Spinel ferrite has formula MFe_2O_4, where M is a divalent cation.

$MgFe_2O_4$ exhibits soft magnetic, high resistivity, non-cytotoxic, and magnetic anisotropy which are lower than of other spinel ferrites because Mg^{2+} is carrying no magnetic moment, so the magnetic coupling is purely originated from the magnetic moment of Fe cations [2, 3]. On the other hand,

$NiFe_2O_4$ exhibits soft magnetic, high resistivity, cytotoxic [2], and magnetic anisotropy which are higher than $MgFe_2O_4$ because Ni^{2+} has a magnetic moment. When Mg^{2+} ions are combined with Ni^{2+} ions with the same composition, $Mg_{0.5}Ni_{0.5}Fe_2O_4$ will be found.

According to properties of ferrites used for biomedical application, ferrite should be biocompatible and non-toxic. Magnetic nanoparticles tend to agglomerate because of their large surface area. Therefore ferrite has encapsulated with organic materials (like chitosan, Polyvinyl alcohol (PVA), Polyethylene glycol (PEG), etc.) or inorganic materials (like gold, silica, etc.) [4]. Silica has silanol groups which can easily react with coupling agents providing strong attachment of surface ligands on magnetic nanoparticles; encapsulated silica increases the stabilization of magnetic nanoparticles in liquid, and it also can prevent agglomeration by increasing the surface charges hence the electrostatic repulses among particles [4]. The silica can produce by using precursor like tetraethyl orthosilicate (TEOS), tetramethyl orthosilicate (TMOS), and sodium silicate (Na_2SiO_3). The precursors like TEOS and TMOS are environmentally unfriendly, toxic, and expensive. Na_2SiO_3 precursors can be used as a source of silica because they are environmentally friendly, non-toxic, and inexpensive [5, 6]. On the other hand, PEG is biocompatible, low-cost, non-toxic, and hydrophilic [7]. PEG with molecular weight under 1000 g/mol is expensive, so PEG-4000 can be used as encapsulation material because it is inexpensive.

Synthesized of $MgNiFe_2O_4$ by coprecipitation has been investigated [8, 9]. In the recent years, the research about silica encapsulated nanocomposites as $NiFe_2O_4$ [10], $KFeO_2$ [11], etc. has gained much attention. PEG also has much attention as encapsulation materials such as for $CaFe_2O_4$ [12], $Mn_{(1-x)}Zn_xFe_2O_4$ [13], etc. However, the study of the influence of silica and PEG encapsulated $Mg_{0.5}Ni_{0.5}Fe_2O_4$ on the structural and magnetic properties has not been paid much attention. In this work, $Mg_{0.5}Ni_{0.5}Fe_2O_4$ will be synthesized by using coprecipitation method and encapsulated by varying the concentration of silica and PEG-4000. The influence of silica and PEG-4000 on crystal structure and magnetic properties of $Mg_{0.5}Ni_{0.5}Fe_2O_4$ will also be investigated.

2. Experimental Method

Two series of silica and PEG-4000 encapsulated magnetic nanoparticle $Mg_{0.5}Ni_{0.5}Fe_2O_4$ were prepared by two steps for each encapsulation materials. Firstly, $Mg_{0.5}Ni_{0.5}Fe_2O_4$ was prepared by using the coprecipitation method. In the second step, silica encapsulated $Mg_{0.5}Ni_{0.5}Fe_2O_4$ was prepared by varying silica concentration along with the using of sodium silicate (SS) precursor. The PEG-4000 encapsulation also prepared by varying PEG concentration. XRD patterns were recorded on Shimadzu XD by using CuK_α radiation. FTIR transmission spectra were taken by using FTIR spectrometer Shimadzu Prestige-21. Magnetic properties of samples were studied by using Vibrating Sample Magnetometer (VSM) Riken Denshi.

2.1. Preparation of magnetic nanoparticle

The magnetic nanoparticle of $Mg_{0.5}Ni_{0.5}Fe_2O_4$ was prepared by coprecipitation method, by using aqueous solutions of magnesium, nickel, and iron salts. The stoichiometric amount of 2.703 g $FeCl_3.6H_2O$ (Merck, Germany) were dissolved in 25 mL of distilled water, 0.508 g $MgCl_2.6H_2O$ (Merck, Germany), and 0.594 g $NiCl_2.6H_2O$ (Merck, Germany) were also dissolved in 25 mL of distilled water and then 3.37 mL HCl was added. The solution was then added in dropwise to 10 M NaOH (Merck, Germany) solution. The reaction was kept under constant stirring at 90˚C for 1 hour. Precipitated ferrite nanopowder was washed with distilled water for six times. Finally, the sample was dried in a furnace at 95 ˚C for 5 hours.

2.2. Silica-encapsulated $Mg_{0.5}Ni_{0.5}Fe_2O_4$

The nanoparticle of $Mg_{0.5}Ni_{0.5}Fe_2O_4$ dissolved to 30 mL silica solution with different concentration (Table 1). Silica solution was prepared by adding sodium silicate to the distilled water stirring at room temperature for 30 minutes. Then, 0.6 g powder of $Mg_{0.5}Ni_{0.5}Fe_2O_4$ was added to silica solution and stirred at room temperature for 5 hours. Encapsulated ferrite was washed by using distilled water for

five times. Finally, the sample was dried at room temperature and then dried in a furnace at 50 ˚C for 30 minutes.

Table 1 Sample of $Mg_{0.5}Ni_{0.5}Fe_2O_4$ with different silica concentration

Sample	$Mg_{0.5}Ni_{0.5}Fe_2O_4$: Silica solution
A	0.6 g : 50% (15 mL SS + 15 mL aquades)
B	0.6 g : 30% (9 mlL SS + 21 mL aquades)
C	0.6 g : 20% (6 mL SS + 24 mL aquades)
D	0.6 g :15% (4.5 mL SS+25.5 mL aquades)
E	0.6 g : 10% (3 mLSS + 27 mL aquades)
F	0.6 g : 5% (1.5 mL SS +28.5 mL aquades)

2.3. PEG-4000 encapsulated $Mg_{0.5}Ni_{0.5}Fe_2O_4$

$Mg_{0.5}Ni_{0.5}Fe_2O_4$ nanoparticles were dissolved in 10 mL of PEG-4000 solution with different concentration (Table 2). The PEG -4000 solution was prepared by adding PEG -4000 to the distilled water stirred at room temperature for 30 minutes. Then, 0.6 g of powder $Mg_{0.5}Ni_{0.5}Fe_2O_4$ was added to PEG-4000 solution and stirred at room temperature for 1 hour. Encapsulated ferrite was washed by using distilled water for five times. Finally, the sample was dried at room temperature.

Table 2 Sample of $Mg_{0.5}Ni_{0.5}Fe_2O_4$ with different PEG-4000concentration

Sample	$Mg_{0.5}Ni_{0.5}Fe_2O_4$: PEG-4000	PEG concentration
G	3:1 (0.6 g : 0.2 g)	25%
H	2:1 (0.6 g : 0.3 g)	33%
I	1:1 (0.6 g : 0.6 g)	50%
J	1:2 (0.6 g : 1.2 g)	67%
K	1:3 (0.6 g : 1.8 g)	75%
L	1:4 (0.6 g : 2.4 g)	80%

3. Results and Discussion

3.1. Silica-Encapsulated $Mg_{0.5}Ni_{0.5}Fe_2O_4$ Nanoparticles

Figure (1a) shows the XRD spectra of $Mg_{0.5}Ni_{0.5}Fe_2O_4$, and (1.b) silica encapsulated of $Mg_{0.5}Ni_{0.5}Fe_2O_4$. The peaks existed in XRD spectra are indexed as (220), (311), (222), and (511) planes. These peaks are the characteristics planes of spinel ferrite (matched with JCPDS card no 36-0398). Figure. 1.a also shows two weak peaks of γ-Fe_2O_3 phase (matched with JCPDS card no 39-1346). The silica encapsulation as depicted in Figure 1b, showed peaks planes of SiO_2 phase (matched with JCPDS card no 45-0131). The silica encapsulation shifted the peak position of (311) to a higher diffraction angle from 35˚ to 36˚ which indicates the decrease of the average lattice spacing due to the strain by the silica. The shift of the (311) peak indicates the existing of the interaction between nanoparticles and silica as the material encapsulation.

As shown in Table 3, the calculated sizes of the $Mg_{0.5}Ni_{0.5}Fe_2O_4$ particles are 5.1 nm, and the encapsulation enlarges to 16.1 nm. The encapsulation provides the nanoparticles begin to react with silica, and hence silica successfully encapsulated the $Mg_{0.5}Ni_{0.5}Fe_2O_4$ nanoparticles [11]. $Mg_{0.5}Ni_{0.5}Fe_2O_4$ nanoparticles became the core and surrounded by silica with a thickness that can manipulate the size of the particle of $Mg_{0.5}Ni_{0.5}Fe_2O_4$. An increase of X-ray density indicates atom density per unit volume at nanoparticles became higher, and the strain value decreases indicating the

reduction of the average lattice spacing due to the appearance of Silica or individual Si and O atoms to nanoparticles.

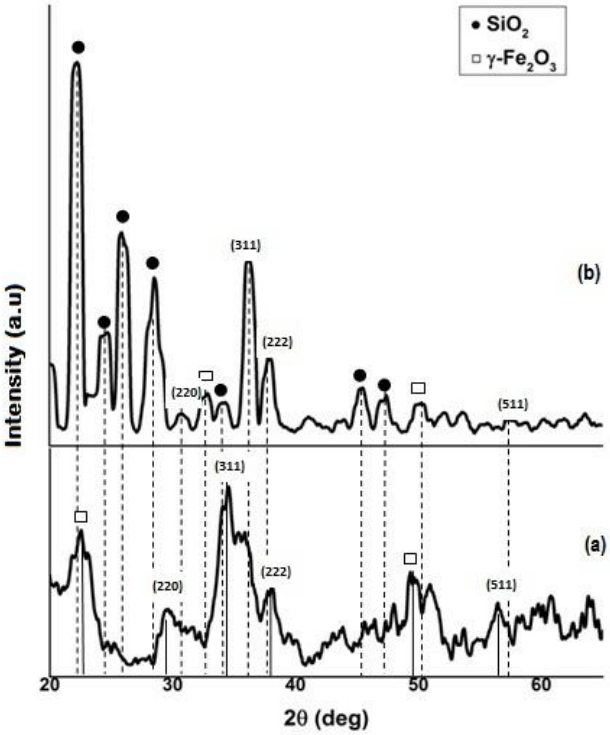

Figure. 1 XRD pattern of (a) $Mg_{0.5}Ni_{0.5}Fe_2O_4$ and (b) silica encapsulated $Mg_{0.5}Ni_{0.5}Fe_2O_4$

Table 3. Data of particles size, lattice parameters, X-ray density, and strain of $Mg_{0.5}Ni_{0.5}Fe_2O_4$ and $Mg_{0.5}Ni_{0.5}Fe_2O_4$ + silica (50%)

Sample	2θ	Lattice parameters (nm)	Particles size (nm)	X-ray density (g/cm^3)	Strain (ε)
$Mg_{0.5}Ni_{0.5}Fe_2O_4$	35	0.85	5.1	4.7	9.2×10^{-2}
$Mg_{0.5}Ni_{0.5}Fe_2O_4$ + Silica (50%)	36	0.82	16.1	5.2	2.8×10^{-2}

The FTIR spectrum of $Mg_{0.5}Ni_{0.5}Fe_2O_4$ at Figure. 2.a shows the bands at 3417.86 cm^{-1} and 1627.92 cm^{-1} are assigned to the O-H stretching and bending vibration, respectively [11, 13, 14]. The bands at 362.62 cm^{-1} correspond to M-O stretching mode of the octahedral group, and 609.51 cm^{-1} corresponds to M-O stretching mode of the tetrahedral group [8, 11, 12]. In the FTIR spectrum of silica (Figure. 2.c) the bands exist at 3487.30 cm^{-1} and 1651.07 cm^{-1} which are assigned to the O-H stretching and bending vibrations. The band at 447.49 cm^{-1} is O-Si-O bending [11, 15, 16], at 794.67 cm^{-1} is Si-OH stretching [11], and at 1087.85 cm^{-1} is Si-O-Si stretching asymmetric [6, 15]. Furthermore, in the FTIR spectrum of silica encapsulated $Mg_{0.5}Ni_{0.5}Fe_2O_4$ nanoparticles (Figure. 2.b) show the bands of nanoparticles and also silica. The bands at 3448.72 cm^{-1} and 1658.78 cm^{-1} are due to O-H stretching and bending vibrations, respectively. The wavenumbers of O-H stretching and bending increase after silica encapsulated $Mg_{0.5}Ni_{0.5}Fe_2O_4$, affected the silica surface is terminated with silanols that have adamant polar interaction. The silanol groups are hydrogen bonded to water and constitute at least part of strongly held water [6]. The O-Si-O bending at 455.2 cm^{-1} [11, 15, 16],

Si-Fe-O at 570.93 cm^{-1} [6, 17], Si-OH stretching at 779.24 cm^{-1} [11], and Si-O-Si stretching asymmetric at 1049.28 cm^{-1} [6, 15] clearly show the presence of silica on $Mg_{0.5}Ni_{0.5}Fe_2O_4$. The bands at 300.9 cm^{-1} and 347.19 cm^{-1} correspond to M-O stretching mode of the octahedral group, and the band at 686.66 cm^{-1} corresponds to M-O stretching mode tetrahedral group [8, 11, 13].

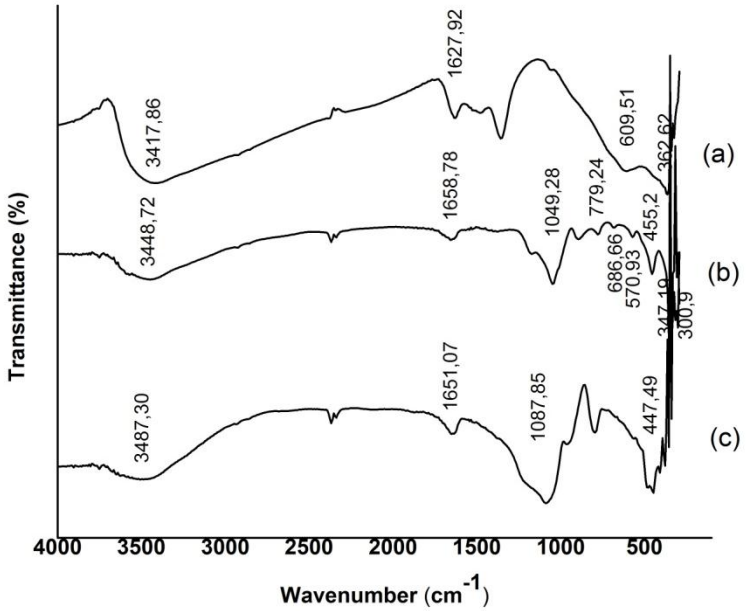

Figure. 2 FTIR spectrum of (a) $Mg_{0.5}Ni_{0.5}Fe_2O_4$, (b) silica encapsulated $Mg_{0.5}Ni_{0.5}Fe_2O_4$, and (c) silica

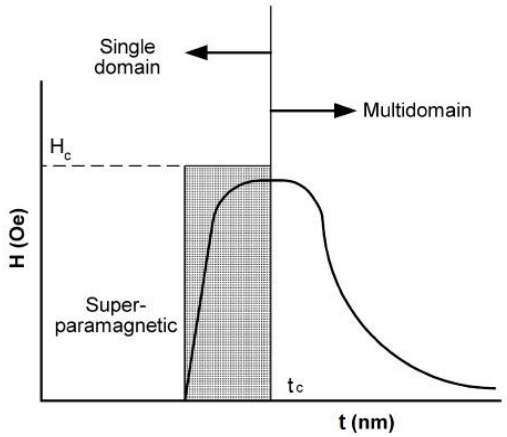

Figure. 3 Illustration of the dependence of coercivity on particle size [1]

Table 4 shown the decrease of coercivity from 47 Oe to 10 Oe affected by increase of silica encapsulation onto $Mg_{0.5}Ni_{0.5}Fe_2O_4$. The coercivity dependence of particle size, if the coercivity is proportional to $1/t$, then the nanoparticles are multidomain. If the coercivity is proportional to t, then the nanoparticles are single-domain. This behavior is illustrated in Figure. 3. Therefore, all samples before and after silica encapsulation are multi-domain due to

the increase of particles size after silica encapsulation. The diamagnetism of SiO_2 phase [1] on nanoparticles also caused coercivity value decreasing as increasing silica concentration. The saturation magnetization of $Mg_{0.5}Ni_{0.5}Fe_2O_4$ was 4.7 emu/g. The saturation magnetization decreased as increasing silica concentration, due to diamagnetism properties of SiO_2 at nanoparticle. SiO_2 caused the magnetic response of $Mg_{0.5}Ni_{0.5}Fe_2O_4$ weaker, so, by increasing silica concentration, the magnetic anisotropy became weaker than before encapsulation.

Table 4. Magnetic parameters at various silica encapsulated $Mg_{0.5}Ni_{0.5}Fe_2O_4$

Sample	Silica concentration (%)	H_c (Oe)	M_s (emu/g)	K (erg/g)
A	50	10	1.0	10
B	30	12	1.1	13
C	20	23	1.8	41
D	15	22	1.6	35
E	10	39	2.0	78
F	5	40	3.2	128
$Mg_{0.5}Ni_{0.5}Fe_2O_4$	0	47	4.7	221

3.2. PEG-4000 Encapsulated $Mg_{0.5}Ni_{0.5}Fe_2O_4$ Nanoparticles

The XRD pattern of $Mg_{0.5}Ni_{0.5}Fe_2O_4$ at Figure 4a shows that it is indexed as (220), (311), (222), and (511), whereas the XRD pattern of PEG-4000 encapsulated $Mg_{0.5}Ni_{0.5}Fe_2O_4$ at Figure. 3.b shows that it is indexed as (311) and (440). After PEG-4000 encapsulation, Figure 4b shows another phase beside $Mg_{0.5}Ni_{0.5}Fe_2O_4$ and γ-Fe_2O_3 phase, that is γ-FeO(OH) phase. Peak position from peak (311) after PEG-4000 encapsulation is shifted to the lower angle from 35˚ to 34.8˚ indicating the increase of the average lattice spacing. The change of the peak position was resulted from the interaction between the nanoparticle and PEG-4000 as material encapsulation. This interaction caused the substituted O atom of O-H group from PEG-4000 to nanoparticles.

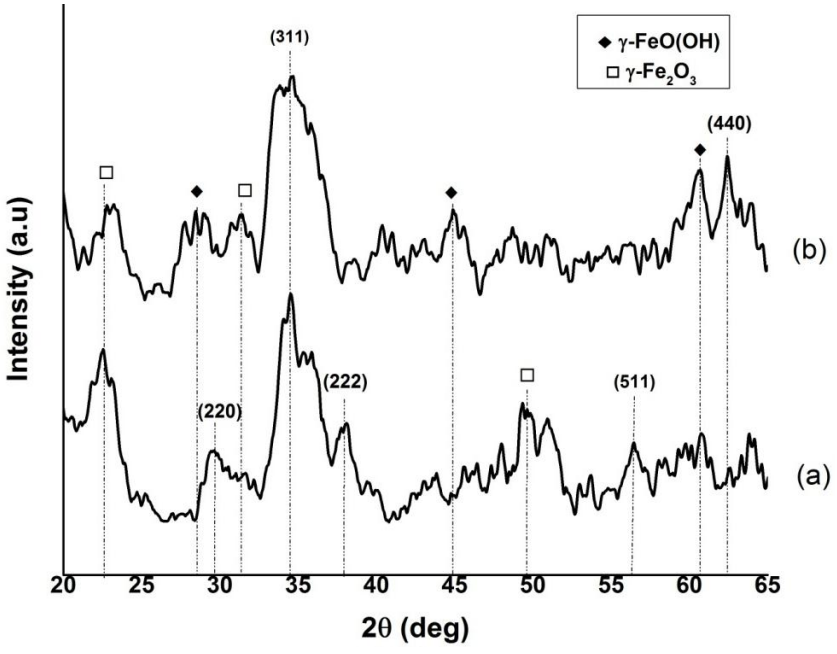

Figure 4. XRD pattern of (a) $Mg_{0.5}Ni_{0.5}Fe_2O_4$ and (b) PEG-4000 encapsulated $Mg_{0.5}Ni_{0.5}Fe_2O_4$

Table 5. Data of particles size, lattice parameters, X-ray density, and strain of $Mg_{0.5}Ni_{0.5}Fe_2O_4$ and $Mg_{0.5}Ni_{0.5}Fe_2O_4$ + PEG-4000 (50%)

Sample	2θ	Lattice parameters (nm)	Particles size (nm)	X-ray density (g/cm^3)	Strain (ε)
$Mg_{0.5}Ni_{0.5}Fe_2O_4$	35	0.85	5.1	4.7	9.2×10^{-2}
$Mg_{0.5}Ni_{0.5}Fe_2O_4$ + PEG-4000 (50%)	34.8	0.86	4.5	4.6	10.2×10^{-2}

Table 5 shows the particles size of $Mg_{0.5}Ni_{0.5}Fe_2O_4$ is 5.1 nm and PEG-4000 encapsulation became 4.5 nm. PEG-4000 has larger molecular weight and a long chain of monomer, so there are a lot of particles trapped by polymer chain and then the growth of crystal decreases and the particle size becomes smaller [18]. Also,Table 5 shows that X-ray density has no significant difference after PEG-4000 encapsulation. Otherwise, the strain became higher than before encapsulation due to the increase of the average lattice spacing because of the substituted O atoms to nanoparticles.

The FTIR spectrum of PEG-4000 (Figure 5c) has bands at 3448.72 cm^{-1} and 1635.64 cm^{-1} which correspond to the O-H stretching and bending vibrations. The bands at 956.69 cm^{-1} is C-H bending (out of plane), at 1465.9 cm^{-1} is C-H in plane bending (scissoring), at 2885 cm^{-1} is C-H stretching (symmetric), and at 1064.71 cm^{-1} and also 1111 cm^{-1} are stretching ether C-O from $–CH_2$-OH group in PEG-4000 [12, 19]. Finally, in the FTIR spectrum of PEG-4000 encapsulated $Mg_{0.5}Ni_{0.5}Fe_2O_4$, (Figure 5b) it shows the bands of PEG-4000 and $Mg_{0.5}Ni_{0.5}Fe_2O_4$. The bands at 3410.15 cm^{-1} and 1627.92 cm^{-1} are assigned to O-H stretching and bending vibrations. The wavenumber of O-H stretching decreases after PEG-4000 encapsulated $Mg_{0.5}Ni_{0.5}Fe_2O_4$ because of PEG-4000 reducing water molecule in nanoparticles. The C-H bending (out of plane) at 925.83 cm^{-1}, C-H in plane bending (scissoring) at 1481.83 cm^{-1}, C-H stretching (asymmetric) at 2924.09 cm^{-1}, and stretching ether C-O at 1103.28 cm^{-1} [12, 19] clearly show the presence of PEG-4000 on $Mg_{0.5}Ni_{0.5}Fe_2O_4$. The bands at 324.04 cm^{-1} and 354.9 cm^{-1} correspond to M-O stretching mode of the octahedral group, and the band at 609.51 cm^{-1} correspond to M-O stretching mode of the tetrahedral group [8, 9, 10].

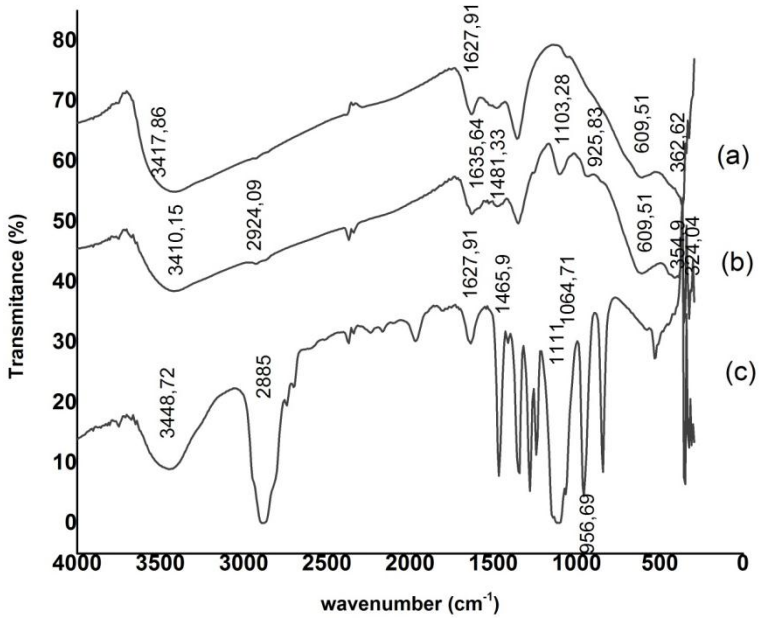

Figure 5. FTIR spectrum of (a) $Mg_{0.5}Ni_{0.5}Fe_2O_4$, (b) PEG-4000 encapsulated $Mg_{0.5}Ni_{0.5}Fe_2O_4$, and (c) PEG-4000

Table 6 shows that the coercivity after PEG-4000 encapsulation has no significant difference with the coercivity of $Mg_{0.5}Ni_{0.5}Fe_2O_4$, which is due to no significant difference in particle size before and after encapsulation that indicates all samples are still in multidomain. The saturation magnetization and magnetic anisotropy increase as increasing PEG-4000 concentration. Increasing of that magnetic parameters is because of the domination $Mg_{0.5}Ni_{0.5}Fe_2O_4$ phase and also because there are two other phases which are γ-Fe_2O_3 and γ-FeO(OH). All phases contributed magnetic moment with different magnetic portion. $Mg_{0.5}Ni_{0.5}Fe_2O_4$ and γ-Fe_2O_3 are ferrimagnetic, and γ-FeO(OH) is antiferromagnetic, so the nanoparticle has random moment magnetic orientation and high magnetic anisotropy.

Table 6. Magnetic Poperties at various PEG-4000 concentration of $Mg_{0.5}Ni_{0.5}Fe_2O_4$

Sample	PEG-4000 concentration (%)	H_c (Oe)	M_s (emu/g)	K (erg/g)
L	80	46	5.8	267
K	75	44	6.1	268
J	67	44	7.6	334
I	50	46	7.7	354
H	33	41	5.7	234
G	25	45	5.7	256
$Mg_{0.5}Ni_{0.5}Fe_2O_4$	0	47	4.7	221

4. Conclusion

The $Mg_{0.5}Ni_{0.5}Fe_2O_4$ nanoparticles have been successfully synthesized by using coprecipitation method. Two series of $Mg_{0.5}Ni_{0.5}Fe_2O_4$ silica encapsulated were prepared at various of the concentration of silica and the concentration of PEG-4000. Silica encapsulation gives rise to produce a new phase, and also change its particle size. The increase of silica encapsulation might reduce the coercivity of $Mg_{0.5}Ni_{0.5}Fe_2O_4$ logarithmically from 47 Oe to 10 Oe which is strongly related to the decline of particle size. The saturation magnetization of $Mg_{0.5}Ni_{0.5}Fe_2O_4$ also decreases from 4.7 emu/g to 1 emu/g as silica increase. On the other hand, it was obtained that the increase of PEG-4000 encapsulation does not alter the coercivity of $Mg_{0.5}Ni_{0.5}Fe_2O_4$ which is due to no significant difference in particle size. This situation was also shown by the saturation magnetization. The saturation magnetization of $Mg_{0.5}Ni_{0.5}Fe_2O_4$ after silica encapsulation also decreases from 4.7 emu/g become 1 emu/g and after PEG-4000 encapsulation the saturation magnetization increases to 7.7 emu/g.

5. References

[1] Mathew D S and Juang R S 2007 *Chemical Engineering Journal* **129** pp 51-56
[2] Khot V M 2013 *Synthesis of Magnesium Merrite Nanoparticles and Studies on Their Induction Heating for Biomedical Applications* (Kolhapur: D. Y. Patil University)
[3] Tomitaka A, Jeun M, Bae S and Takemura Y 2011 *Journal of Magnetics* **16(2)** pp 164-168
[4] Umut E 2013 *Surface Modification of Nanoparticles Used in Biomedical Applications* In Tech, chapter 8 pp 185-208
[5] Setyawan H and Balgis R 2011 *Asia-Pac. J. Chem. Eng* **7** pp 448-454.
[6] Setyawan H, Fajaro F, Widiyastuti W, Winard, Sugeng I, Lenggoro, Wuled and Nandang M., 2012 *J Nanopart Res* **14** 807
[7] Covaliu C I, Jitaru I, Paraschiv G, Vasile E and Biris S S 2013 *Powder Technology* **273** pp 415-426
[8] Hankare P P, Jadhav S D, Sankpal U B, Chavan S S, Waghamare K J and Chougule B K 2009 *Journal of Alloys and Coumpounds* **475** pp 926-929
[9] Moradmard H, Shayesteh S F, Tohidi P, Abbas Z and Khaleghi M 2015 *Journal of Alloys and Coumpounds* **650** pp 116-122

[10] Nadeem K, Krenn H, Sarwar W and Mumtaz M 2014 *Applied Surface Science* **288** pp 677-681
[11] Khanna L and Verma N K 2013 *Materials Science and Engineering* ***B*** **178** pp 1230-1239
[12] Khanna L and Verma N K 2013 *Physica* ***B*** **427** pp 68-75
[13] Kareem S H, Ati A A, Shamsuddin M and Lee S L 2015 *Ceramic International* **41** pp 11702-11709
[14] Ahmadipour M, Mohzhgan H and Kalagadda V R 2012 *Advances in Nanoparticle* **1** pp 37-43
[15] Mojić B, Giannakopoulos K P, Cvehić Ž and Srdić V V 2012 *Ceramic International* **38** pp 6635-6641
[16] Gharagozlou M, Naderi R, and Baradaran Z 2016 *Progress in Organic Coating* **90** pp 407-413
[17] Zhang S, Dong D, Sui Y, Liu Z, Wang H, Qian Z and Su W 2006 *Journal of Alloys and Compounds* **415** pp 257-260
[18] Perdana F A, Baqiya M A, Mashuri, Triwikantoro and Darminto 2011 *Jurnal Material dan Energi Indonesia* **01** pp 1-6
[19] Pavia D L, Lampman G M, Kriz G S, and Vyvyan J R 2009 *Introduction to Spectroscopy Fourth Edition* (USA: Brooks/Cole Cengage Learning)

Acknowledgements
The reported work was financially supported by *Hibah Kompetensi* (HIKOM) from the Ministry of Research and Technology of High Education for the period of 2015 – 2017 and Nanofabrication Platform Consortium Project of Nagoya University, Minister of Culture, Sport, Science and Technology (MEXT) Nano-Project Platform, Japan for the Period of 2012-2016.